ACS Partner Journal

Journal of the American Society for Mass Spectrometry

pubs.acs.org/jasms

Research Article

Implementing Digital-Waveform Technology for Extended *m/z* Range Operation on a Native Dual-Quadrupole FT-IM-Orbitrap Mass Spectrometer

Jacob W. McCabe,[⊥] Benjamin J. Jones,[⊥] Thomas E. Walker,[⊥] Robert L. Schrader, Adam P. Huntley, Jixing Lyu, Nathan M. Hoffman, Gordon A. Anderson, Peter T. A. Reilly, Arthur Laganowsky, Vicki H. Wysocki, and David H. Russell*

Cite This: *J. Am. Soc. Mass Spectrom.* 2021, 32, 2812−2820

Read Online

ACCESS | Metrics & More | Article Recommendations | Supporting Information

ABSTRACT: Here, we describe a digital-waveform dual-quadrupole mass spectrometer that enhances the performance of our drift tube FT-IMS high-resolution Orbitrap mass spectrometer (MS). The dual-quadrupole analyzer enhances the instrument capabilities for studies of large protein and protein complexes. The first quadrupole (q) provides a means for performing low-energy collisional activation of ions to reduce or eliminate noncovalent adducts, viz., salts, buffers, detergents, and/or endogenous ligands. The second quadrupole (Q) is used to mass-select ions of interest for further interrogation by ion mobility spectrometry and/or collision-induced dissociation (CID). Q is operated using digital-waveform technology (DWT) to improve the mass selection compared to that achieved using traditional sinusoidal waveforms at floated DC potentials (>500 V DC). DWT allows for increased precision of the waveform for a fraction of the cost of conventional RF drivers and with readily programmable operation and precision (Hoffman, N. M. et al.. A comparison-based digital-waveform generator for high-resolution duty cycle. *Review of Scientific Instruments* **2018**, *89*, 084101).

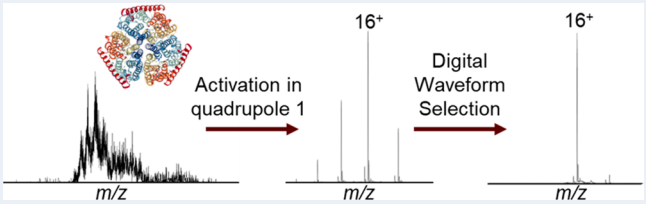

KEYWORDS: *native mass spectrometry, Fourier-transform ion mobility-Orbitrap mass spectrometry, digital-waveform technology, quadrupole mass spectrometry*

INTRODUCTION

Studies of proteins, protein complexes, and noncovalent protein−ligand interactions using native mass spectrometry have expanded the structural biology toolbox. Often quoted attributes ascribed to native MS are sensitivity and dynamic range, which makes possible studies of reaction products, including intermediates on the pathway from initial reactant to final products.[1,2] Native MS is highly complementary to the traditional structural biology techniques, i.e., cryogenic electron microscopy,[3,4] X-ray crystallography,[5,6] and NMR spectroscopy.[7,8] While the working mass range, mass resolution, and mass measurement accuracy for large 100 kDa and even MDa protein complexes have increased dramatically over the past decade, there remain significant challenges to developing advanced technologies for structure-based MS studies that complement existing structure analysis methods.[9]

We recently described an Orbitrap IM-MS instrument consisting of a periodic focusing drift tube (PF-DT) IM and Orbitrap mass analyzer specifically designed for studies of large proteins and protein complexes.[10−15] The PF-DT IM system affords first-principle determinations of rotationally averaged ion-neutral CCS,[11,16] and the Orbitrap extended mass range (EMR) mass analyzer affords high-mass resolving power (R_P) of ions up to 20 000 *m/z* and, when combined with a variable temperature (vT)-ESI source (T variable from 5−95 °C), affords studies of the thermodynamics (ΔG, ΔH, and ΔS) of protein/protein complex, folding/refolding, as well as ligand−protein and ligand-protein complex interactions.[17] Here, we describe an additional modification to the PF-DT-FT-IMS-Orbitrap, viz., incorporating a dual-quadrupole (qQ) mass analyzer positioned between the vT-ESI source and the IM drift tube, which further enhances our capabilities for structural characterization of large proteins and protein complexes. The first quadrupole (q) is operated as an ion guide (RF-only mode) and can also be used for mild collisional activation of the ions to remove unwanted adducted species (H_2O, salts, detergents, and charge reducing reagents). The second quadrupole (Q) is used for mass selection and is operated

Received: August 17, 2021
Revised: October 19, 2021
Accepted: November 12, 2021
Published: November 19, 2021

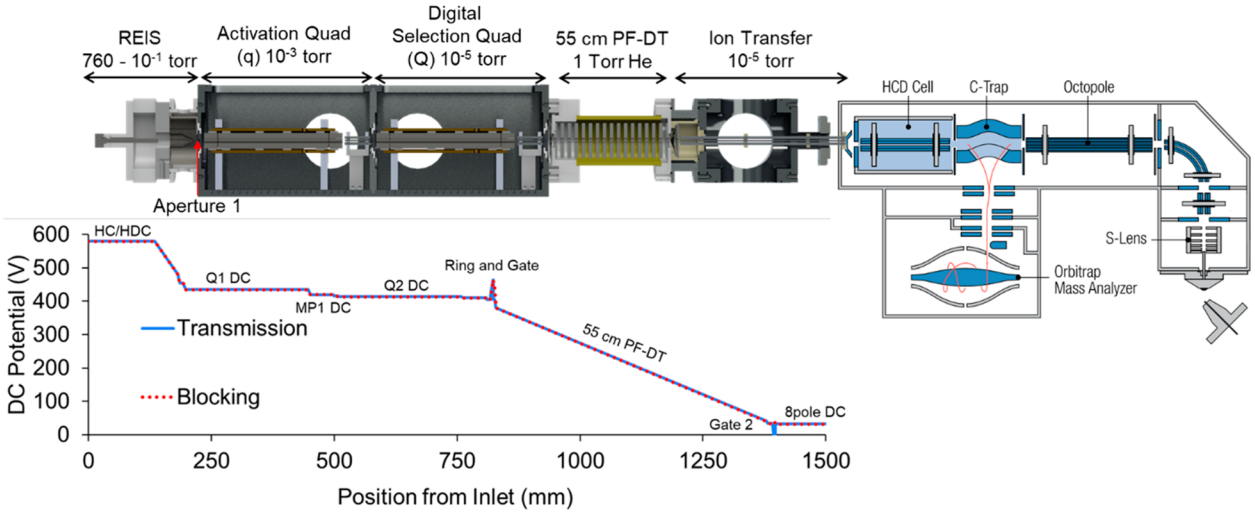

Figure 1. SolidWorks rendering of the nano-ESI dual-quadrupole FT-IM-PF-DT coupled to the HCD cell of a Thermo Exactive Plus Orbitrap with Extended Mass Range (qQ-FT-IM-PF-DT-HCD Orbitrap) with the major components labeled and the applied DC potential gradient across the instrument. The length of the DT is not to scale in the rendering, i.e., the vacuum box and qQ are enlarged to illustrate this device better; the DT, 8-pole, and other ion optics have been described previously.[12]

using digital-waveform technology (DWT) developed in the Reilly laboratory.[18−32] The modular design of the instrument allows for the installation of additional ion activation techniques, such as surface-induced dissociation (SID),[33−37] electron transfer/capture dissociation (ETD/ECD),[38] and ultraviolet photodissociation (UVPD)[39,40] prior to IM-MS characterization. Collectively, the experimental versatility of the (vT)-nESI-qQ-PF-DT-FT-IM-Orbitrap increases our research capabilities for native-mass-spectrometry-guided structural biology. Below, we describe these advantages and the ability to analyze complex membrane protein complexes through removal of nonspecific adducts such as lipids and salts.[28] We demonstrate the ability of the DWT Q to select individual charge states of protein complexes up to 12 500 m/z.[22,27,29] Lastly, we show IM data and the ability to perform complex-down sequencing and analysis of proteins. The new capabilities of this instrument facilitate the ability to analyze complex systems with its plethora of analysis methods afforded by the modularity of the instrument design.

■ EXPERIMENTAL SECTION

Methods. Human recombinant C-reactive protein (CRP, 1 mg in 140 mM NaCl, 20 mM Tris-HCl, 2 mM $CaCl_2$, 0.05% NaN_3, at a pH of 7.5), ammonium transport channel, AmtB, and GroEL were expressed and purified as previously described.[10,41−44] The proteins were buffer exchanged using Micro Bio-Spin *P*-6 Gel Columns (Bio-Rad) into 200 mM ammonium acetate, and working concentrations were adjusted to 1 to 5 μM. A 5 μL aliquot of protein was backloaded into pulled borosilicate tips prepared in-house from borosilicate capillaries (Sutter Instruments, BF150−86−10) using a micropipette puller (Sutter Instruments, P1000).

Instrumentation. The PF-DT-FT-IM Orbitrap has been described previously,[10−13,17] and the latest iteration of the instrument, including the qQ module, is shown in Figure 1. The qQ-PF-DT-FT-IM-Orbitrap configuration consists of a reverse-entry ion source (REIS) that has been previously described.[45] The REIS source is mounted onto an aluminum vacuum chamber (designed and fabricated in-house). The vacuum chamber is divided into two differentially pumped regions and pumped by a two-stage, split flow turbomolecular vacuum pump (Pfeiffer TMH 261−250−010 P3P). The first vacuum chamber (maintained at ∼10^{-3} Torr) houses a 250 mm hyperbolic quadrupole (q) that is operated in a transmission/focusing mode and can also be tuned for collisional activation (CA). Collisional activation is achieved by raising the potentials on all optics up to and including the conductance limit into the q chamber; activation voltage is defined as the potential difference between the previous aperture and the quadrupole 1 DC bias. The ions exiting q are guided to the second chamber by an octupole ion guide constructed from 3.175 mm rods with a 4.75 mm r_0 measuring 47 mm in length and enter a 250 mm hyperbolic quadrupole (Q) that is maintained at 10^{-4}−10^{-5} Torr. Q is used to mass-select the ions by digital-waveform technology (DWT) as described and developed by the Reilly laboratory.[18−32] Both quadrupoles are identical Thermo Fisher 4 mm r_0 hyperbolic rods with pre- and postfilters (Part Number 80100−60109); quadrupole pre- and postfilters were wired directly to the main rods prior to use. All the experiments described below employ the DWT operation of the Q MS. Ions exiting Q enter an octupole ion guide (47 mm) and then transfer to a 55 cm PF-DT maintained at pressures of 1−2 Torr of He. The DT-IMS is operated in the FT-IMS mode as described previously.[12,46−51] The ions exiting the DT enter a final octupole ion guide and are transferred to the HCD cell of the Orbitrap mass spectrometer, as described previously.[12]

The DC voltages used in this work are provided by a Modular Intelligent Power Sources (MIPS) system (GAA Custom Engineering Kennewick, WA) and Ortec 710 Quad 1 kV power supply. Confining RF voltages for the ion funnel, octupoles in the dual-quad system, and transfer octupole are driven using MIPS RF High Q Heads at 200 V_{pp} 440 kHz, 200 V_{pp} 650 kHz, 250 V_{pp} 700 kHz, respectively. The transmission quadrupole "q" in the activation region is driven by a MIPS Ultra RF head ∼1.15 MHz 150−350 V_{pp} tuned for each system. The mass selection quadrupole ("Q") utilizes a custom-built comparison-based control system capable of a

https://doi.org/10.1021/jasms.1c00245
J. Am. Soc. Mass Spectrom. 2021, 32, 2812−2820

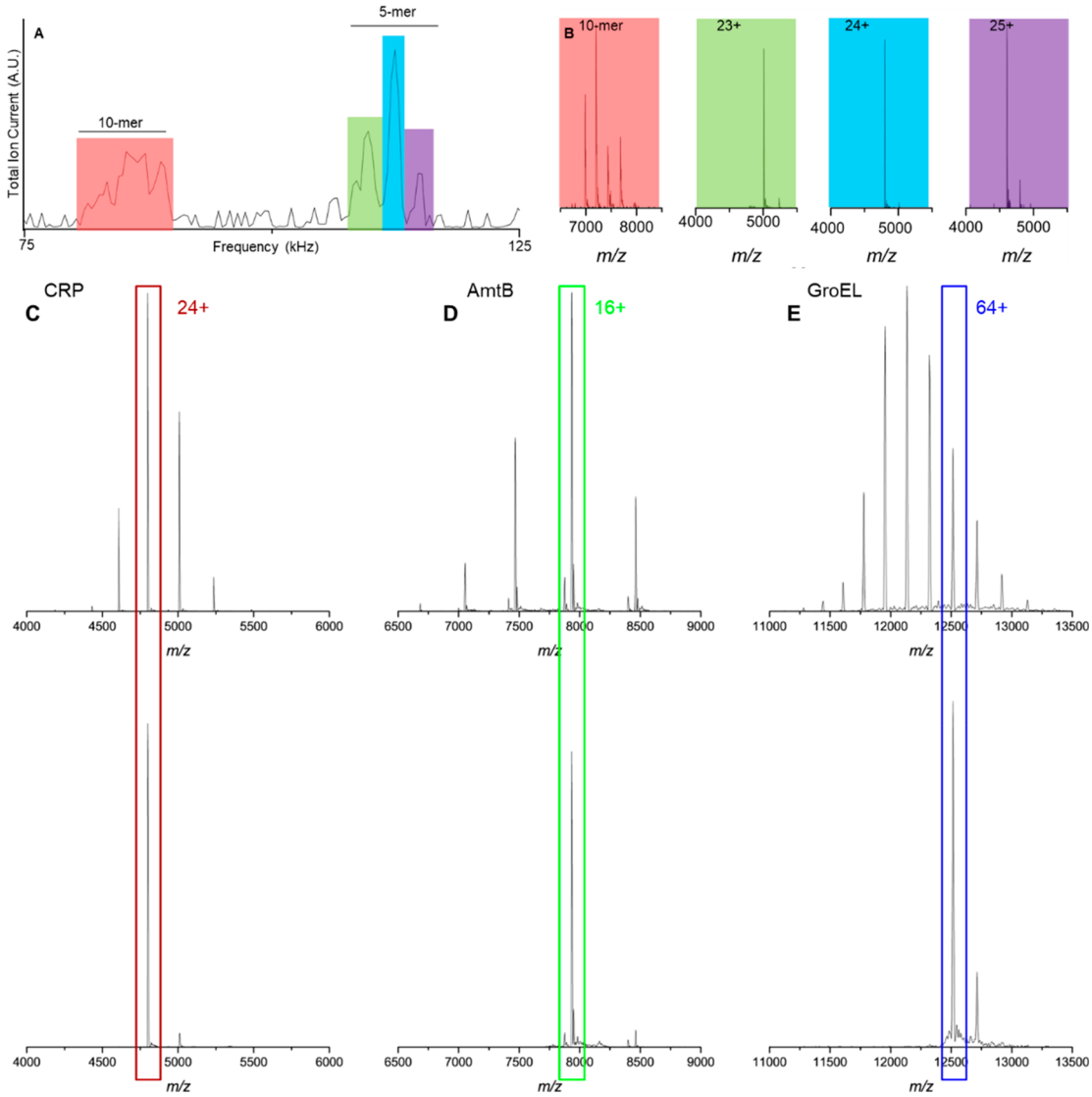

Figure 2. (A) Total ion current (TIC) detected as the frequency of Q (85/15 duty cycle with a ±10 V DC bias applied on rod pairs at 300 V_{pp}) is increased from 75 to 125 kHz. Frequency stepped in 1 kHz steps at the rate of 1 kHz per second in panel A to produce an m/z selection chromatogram of quadrupole 2 (Q). (B) Extracted MS for the given frequency range shown in panel A. Full-ion transmission and isolation of a single charge state for CRP (panel C), AmtB (panel D), and GroEL (panel E).

high-resolution duty cycle control designed by the Reilly group,[23] fabricated by PCBPrime (Aurora, CO), and assembled at Texas A&M University. Briefly, digital-waveform technology (DWT) utilizes two rectangular waves with a varying duty cycle (defined as the percent in a given period that the wave spends in the "High" versus "Low" state) to manipulate ions on the Mathieu stability diagram. Isolation is obtained by tuning the duty cycle to vary the resolution and access higher stability zones and then sweeping the frequency of the waveforms by making an ion of interest stable in both the *X*- and *Y*-planes. This mode of mass selection has been demonstrated by Opačić et al. for lysozyme (14.3 kDa monomeric protein) by applying a 75% duty cycle to the *X*-waveform and a 25% duty cycle to the *Y*-waveform (i.e., a 75/25 duty cycle).[28] This waveform allows mass analysis in stability zone B, as previously described.[29] DWT was implemented due to the high electric fields pre-IM where the DC bias of Q is elevated ∼500 V above ground, without the added cost or complexity of using a traditional high-mass sinusoidal quadrupole driver.[52] The DC voltage is applied to the quadrupole using a set of DC-RF coupling circuits designed and fabricated by GAA Custom Electronics.

Data Processing. IM data files were processed as previously described.[12,14] Custom Python code utilized *multiplierz*[53] to process Thermo RAW files over the entire acquisition. IM-MS data were obtained by deconvoluting Fourier transform IM and converted from frequency to drift time domains using SciPy[54] and NumPy.[55] The resulting set of data is then imported into UniDec[56] or Protein Metrics[57] for additional processing.

■ RESULTS AND DISCUSSION

Previously, mass selection with DWT has only been experimentally achieved for small, non-native proteins[28] but has been simulated for complexes approaching MDa masses.[24−27,31] In this work, the mass selection of individual charge states for large protein complexes (>100 kDa) has been effectuated. The overall performance of DWT for isolation of

https://doi.org/10.1021/jasms.1c00245
J. Am. Soc. Mass Spectrom. 2021, 32, 2812−2820

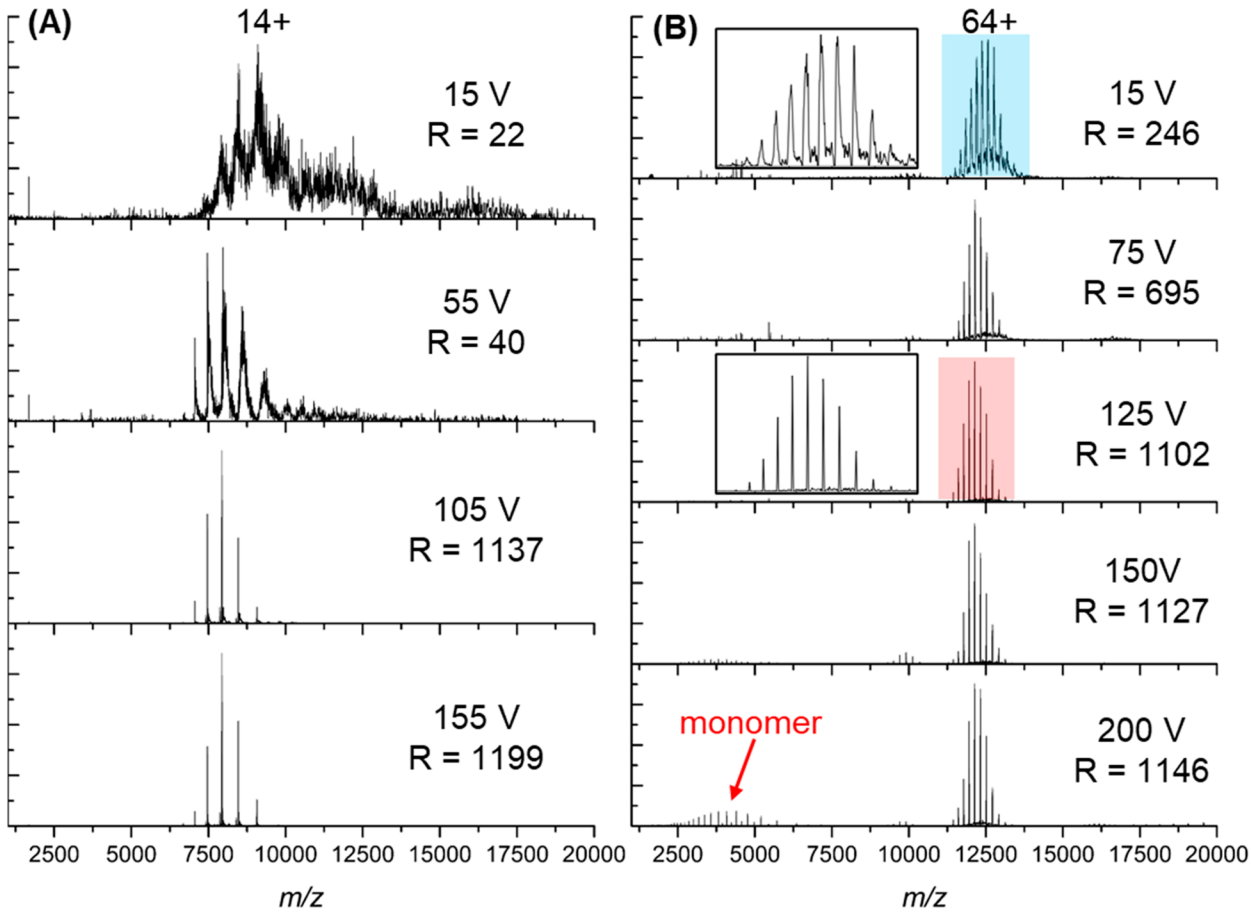

Figure 3. Mass spectra illustrating how mild collisional activation in the q of the qQ-FT-IM-PF-DT Orbitrap can be used to remove adducted species (salts, endogenous lipids, and other small molecules) from (A) the trimeric ammonia transport channel (AmtB, 127 kDa) and (B) GroEL (801 kDa, tetradecamer (n = 14)). The collision voltages indicated refer to the potential differences between the exit of the ion funnel and the time-averaged DC potential of the activation quad, q at various DC potential drops. Collisional activation in q may produce non-native state ions; whether this occurs or not can be assessed by using ion mobility, as shown in panels B and C of Figure 4. The resolution (denoted R based on fwhm) for the most abundant charge state is listed in each panel. The insets in (B) more clearly illustrate the higher resolving power following collisional activation in q for the GroEL tetradecamer.

single charge states of C-reactive protein (CRP), membrane protein ammonium transport channel (AmtB), and type 1 chaperonin GroEL is illustrated by data shown in Figure 2. This data was collected using a highly asymmetric duty cycle of 85/15 to generate the waveform in Q. Transmission for all ions is generally achieved at a 50/50 duty cycle; more asymmetric duty cycles (such as 60/40, 75/25, 85/15) produce a narrowing window of stability in the m/z dimension. The positioning of this selection window in the m/z dimension is controlled by the DWT frequency applied to Q, as reported previously.[22] Thus, scanning the frequency of a requisitely narrow stability window should give rise to individual charge states as a function of the applied frequency in the DWT. Figure 2A exhibits this frequency scanning procedure for a sample of CRP scanned from 75 to 125 kHz. Note the low abundance of the total ion current (TIC) at low frequencies (75 kHz), which indicates the low-mass cutoff (LMCO) is above the lowest charge state of the decamer, resulting in no ion transmission. As the frequency increases, stability zones are reached to allow for the transmission of the CRP decamer charge state distribution. These signals then dissipate as the frequency increases, signifying that the frequencies in the middle of the plot do not stabilize any of the observed species. Around 100 kHz in Q, the first signals for the CRP pentamer begin to appear; each of the subsequent peaks in Figure 2A are a result of stabilizing individual charge states for the CRP pentamer (m/z 5008 (23^+), m/z 4779 (24^+), m/z 4609 (25^+), respectively). The TIC peaks are extracted and displayed as mass spectral plots in Figure 2B, demonstrating the selection of individual charge states in Q.

Isolation of other model protein complexes is executed by repeating the frequency sweep for selecting a single CRP charge state. Figure 2C−E illustrates the selection capabilities of Q using model protein systems CRP, AmtB, and GroEL. With the isolation of a single-charge state for these complexes and with support by previous theory, evidence suggests that the (3,1) stability zone (the intersection of the third stability zone along the X-axis and first stability zone on the Y-axis) can be accessed without a significant loss in throughput or sensitivity.[58] Collectively, the data shown in Figure 2 illustrate the isolation of a single charge state of native protein complexes CRP (115 kDa), AmtB (127 kDa), and GroEL (801 kDa), thereby making it possible to perform more detailed experiments, IMS, CID, both top-down and complex-down, on specific charge states of proteins and protein complexes.

https://doi.org/10.1021/jasms.1c00245
J. Am. Soc. Mass Spectrom. 2021, 32, 2812−2820

The performance of the qQ-FT-IMS-Orbitrap mass spectrometer was evaluated using protein complexes that illustrate specific requirements for a variety of native MS research projects. Native mass spectra of membrane protein complexes contain abundant signals that arise from nonspecific adducts, i.e., detergents and/or salts on the protein carried over during the ESI process.[59,60] The qQ quadruple system is used to implement mild collisional activation of complexes to remove these adducted species. For example, AmtB is a membrane protein that requires solubilization in detergent micelles for MS compatibility.[42,43,61−65] Figure 3A contains the mass spectrum of AmtB with the detergent micelle C_8E_4 (tetraethylene glycol monooctyl ether) and other adducts prior to collisional activation.[66] Increasing the potential drop between the ion funnel to 55 V provides sufficient collisional activation to remove some of the adducted molecules.[67] A further increase in the collision energy provides more narrow peaks and shifts in the average charge states. Similar effects of mild activation are observed for GroEL (Figure 3B), where initially endogenous adducts are bound to GroEL at low activation voltages (e.g., 15 V).[11,68] As the activation voltage is increased to 125 V for GroEL, the nonspecific adducts are removed. The activation in q results in baseline-resolved charge states shown by the resolution increase from 246 to 1102 at 15 and 125 V, respectively. However, as activation energy increases beyond 125 V, the GroEL tetradecamer dissociates to form monomers and tridecamers at low abundance.

Increased activation energy raises concerns regarding possible structural rearrangements that may occur, specifically collision-induced unfolding (CIU). Note changes in the peak profiles for GroEL (Figure 3B) that show shifts to a higher average charge state (Z_{avg}) when the activation energy is increased. At 15 V of activation, the average charge state—as measured by UniDec—is calculated to be 64.63^+, compared to Z_{avg} shifts to 65.88^+ at 125 V. The shifts in Z_{avg} could occur by loss of negatively charged adducts that might also be accompanied by structural changes.

Questions regarding possible CIU accompanying collision activation are better answered by experimental CCS measurements. Data shown in Figure 4A were collected using DT field strengths of 5.80 $V \cdot cm^{-1} \cdot torr^{-1}$ and in He bath gas as described previously.[11] The CCS for the CRP pentamer and decamer ions of 6.3 nm^2 (23^+) and 8.9 nm^2 (31^+) formed using low collisional activation conditions (20 V) are consistent with measurements reported by Wysocki et al. (see the SI for a complete list of CCS values).[69] Figure 4B contains ATD vs m/z plots for the GroEL tetradecamer obtained using an activation voltage of 100 V; under these conditions, the intact $GroEL_{14}$ ions do not appear to be broadened by the presence of adducts. The measured CCS value of 225.1 nm^2 (64^+, 200 mM ammonium acetate buffer) obtained using a field strength of 4.54 $V \cdot cm^{-1} \cdot torr^{-1}$ is ∼5.9% smaller than the previously reported value of 239.2 nm^2.[11] While these differences may be interpreted as evidence that collisional activation promotes conformational changes, we feel this interpretation is premature and must be explored further. All previously reported CCS values for GroEL were obtained for ions that are known to have unknown numbers of adducts, salts, small molecules, possibly including water; consequently, these discrepancies may be due solely to the presence of endogenous adducts. Another consideration is the differences for the measured (807 kDa) and predicted mass (801 kDa) of the GroEL complex—a small error of ∼1%. Further studies using both single-domain proteins and protein complexes are currently underway.

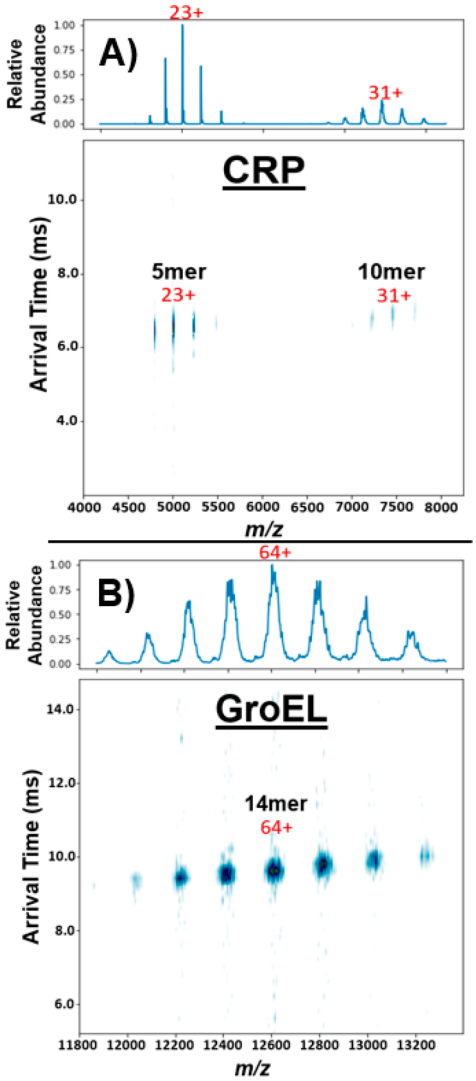

Figure 4. Mass spectra and IMS arrival-time distribution plots for (A) pentamer and decamer complexes of C-reactive protein (CRP) and (B) the tetradecamer GroEL chaperone.

Complex-Down Characterization of a Protein Complex (C-Reactive Protein (CRP)). The configuration of the instrument provides additional avenues for structural native MS.[70,71] For example, activation in q can be used to dissociate protein complexes thereby forming ($n - x$) oligomers and even monomers, and these products can be analyzed by either ion mobility or by CID in the HCD cell of the Orbitrap MS. Figure 5A contains CID products obtained using a range of activation voltages in q. Using mild activation energies (∼15 V), the mass spectrum of CRP contains abundant ions corresponding to the native, intact pentamer of CRP (115 kDa) and low-abundance signals for the decamer. Increasing the activation voltage to 55 V promotes dissociation of both the CRP pentamer and dodecamer into the respective monomer and tetramer ions and further increases in the activation voltage (105 and 155 V), producing monomer, tetramer, and nonomer ions. Mass selection of the specific CID products formed in q can be performed by DWT operation of Q, and the mass-selected ions can then be analyzed by CID in

https://doi.org/10.1021/jasms.1c00245
J. Am. Soc. Mass Spectrom. 2021, 32, 2812−2820

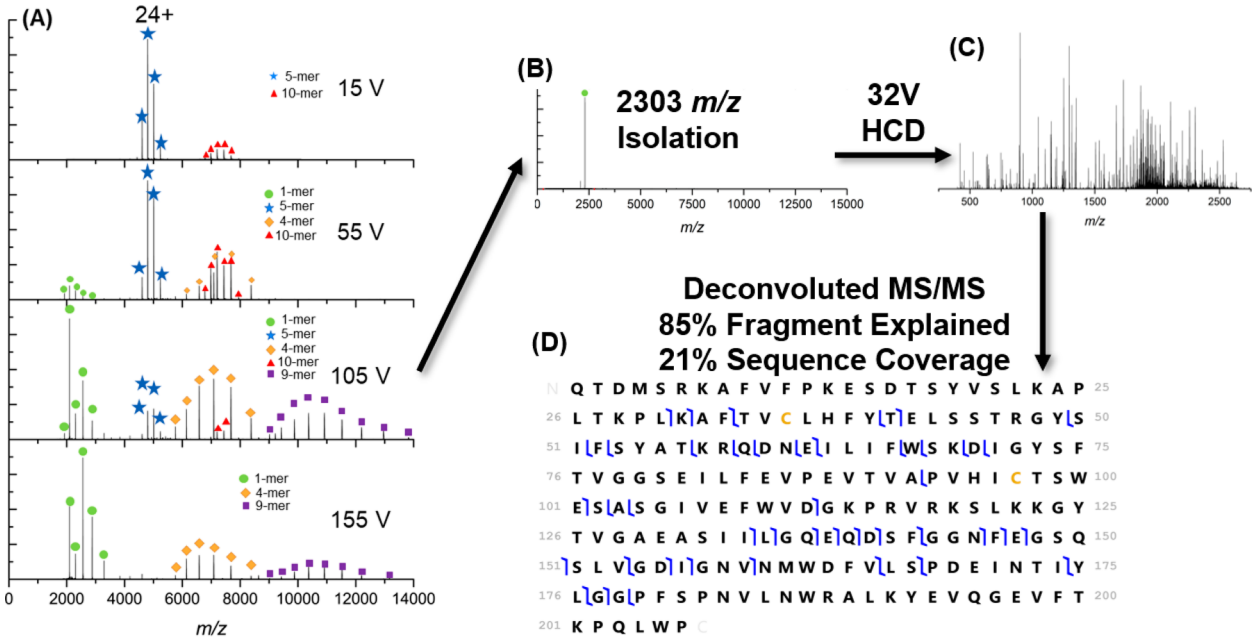

Figure 5. Complex-down characterization of the CRP. (A) The native MS spectrum of CPR is shown in the top panel, and each of the panels below contains mass spectra resulting from collisional activation (at the indicated voltage) of the ion populations in the panel above. Panel (B) contains the mass spectrum obtained by using DWT to mass-select the CRP monomer (24^+ pentamer ion), and panel (C) contains the top-down mass spectrum of the mass-selected ion shown in panel (B). The amino acid sequence of CRP is shown, and the sequence informative fragment ion is labeled accordingly in panel (D).

the HCD cell of the Orbitrap MS (resolving power setting: 140 000 at 200 m/z), illustrated in Figure 5B–D. The fragment ions formed in this manner, a pseudo-MS^3 sequence, were deconvoluted using UniDec,[56] ProteinMetrics,[57] and ProSite Lite[72] to achieve top-down sequencing of the protein. This approach provided ~21% sequence coverage for the 10^+ monomer ions, where 80% of the detected fragments are assignable. The sequence coverage for the 12^+ monomer ions increased to 31%, with 85% assigned fragments (data not shown). The mass resolving power of the Orbitrap mass analyzer, which provides isotopic resolution, affords higher confidence for assignments of the high-charge fragments.[73]

CONCLUSIONS

A high-resolution digital-waveform programmable dual-quadrupole FT-IM Orbitrap is described, and capabilities of this approach for activation and mass selection for IM-MS analysis and complex-down analysis of large protein complexes are demonstrated. The ability to perform collisional activation of ions formed by native ESI prior to mass filtering to desolvate and remove nonspecific adducts is demonstrated for a membrane protein complex (AmtB, 127 kDa) and a chaperone protein complex (GroEL, 801 kDa). Operating quadrupoles at high DC voltages is challenging owing to safety concerns and the high cost of RF drivers; however, these complications are alleviated using modern digital-waveform technologies. Additional activation techniques (e.g., CID, ECD/ETD, and SID) can be added to this platform to expand the current platform to probe subunit interfaces. Notably, for the first time, DWT has been shown to transmit, isolate, and filter large protein complexes (approaching the MDa size) supporting the previously described theory.[58]

ASSOCIATED CONTENT

Supporting Information

The Supporting Information is available free of charge at https://pubs.acs.org/doi/10.1021/jasms.1c00245.

Figure S1. CCS data for the CRP pentamer, decamer, and GroEL tetradecamer; Table S1. Relevant values used to calculate the CCS of the CRP pentamer, decamer, and GroEL tetradecamer (PDF)

AUTHOR INFORMATION

Corresponding Author

David H. Russell – *Department of Chemistry, Texas A&M University, College Station, Texas 77842, United States;* orcid.org/0000-0003-0830-3914; Email: russell@chem.tamu.edu

Authors

Jacob W. McCabe – *Department of Chemistry, Texas A&M University, College Station, Texas 77842, United States;* orcid.org/0000-0002-5022-2280

Benjamin J. Jones – *Department of Chemistry and Biochemistry, The Ohio State University, Columbus, Ohio 43210, United States;* orcid.org/0000-0002-6135-4377

Thomas E. Walker – *Department of Chemistry, Texas A&M University, College Station, Texas 77842, United States*

Robert L. Schrader – *Department of Chemistry, Texas A&M University, College Station, Texas 77842, United States*

Adam P. Huntley – *Department of Chemistry, Washington State University, Pullman, Washington 99164, United States;* orcid.org/0000-0002-2866-0217

Jixing Lyu – *Department of Chemistry, Texas A&M University, College Station, Texas 77842, United States*

Nathan M. Hoffman – *Department of Chemistry, Washington State University, Pullman, Washington 99164, United States*

https://doi.org/10.1021/jasms.1c00245
J. Am. Soc. Mass Spectrom. 2021, 32, 2812–2820

Gordon A. Anderson − *GAA Custom Electronics, Kennewick, Washington 99338, United States*
Peter T. A. Reilly − *Department of Chemistry, Washington State University, Pullman, Washington 99164, United States;* orcid.org/0000-0001-7679-4511
Arthur Laganowsky − *Department of Chemistry, Texas A&M University, College Station, Texas 77842, United States;* orcid.org/0000-0001-5012-5547
Vicki H. Wysocki − *Department of Chemistry and Biochemistry, The Ohio State University, Columbus, Ohio 43210, United States;* orcid.org/0000-0003-0495-2538

Complete contact information is available at: https://pubs.acs.org/10.1021/jasms.1c00245

Author Contributions

[⊥]J.W.M., B.J.J., and T.E.W. contributed equally to this work

Notes

The authors declare the following competing financial interest(s): The power supplies used for this instrument were purchased from G.A.A. Custom Electronics, owned by a co-author (G.A.A.). Other authors declare no competing financial interests.

■ ACKNOWLEDGMENTS

The authors would like to thank William Seward and Karl Yeager of the Texas A&M University Chemistry Machine Shop for the fabrication of the parts, Dr. Andrew Roth and Dr. Hays Rye for providing the GroEL sample, and Dr. Alexander Makarov and Dr. Kyle Fort for the assistance in the initial development of the REIS. Funding for this work was provided by the National Science Foundation CHE-1707675 (D.H.R.), National Institutes of Health DP2GM123486 (A.L.), R01GM121751 (D.H.R. and A.L.), and P41GM1285771 (D.H.R. and V.H.W.) and endowment funds from an MDS SCIEX Professorship (D.H.R.).

■ REFERENCES

(1) Clemmer, D. E.; Russell, D. H.; Williams, E. R. Characterizing the Conformationome: Toward a Structural Understanding of the Proteome. *Acc. Chem. Res.* **2017**, *50* (3), 556−560.
(2) McCabe, J. W.; Hebert, M. J.; Shirzadeh, M.; Mallis, C. S.; Denton, J. K.; Walker, T. E.; Russell, D. H. THE IMS PARADOX: A PERSPECTIVE ON STRUCTURAL ION MOBILITY-MASS SPECTROMETRY. *Mass Spectrom. Rev.* **2021**, *40* (3), 280.
(3) Bai, X.-C.; McMullan, G.; Scheres, S. H. W. How cryo-EM is revolutionizing structural biology. *Trends Biochem. Sci.* **2015**, *40* (1), 49−57.
(4) Murata, K.; Wolf, M. Cryo-electron microscopy for structural analysis of dynamic biological macromolecules. *Biochim. Biophys. Acta, Gen. Subj.* **2018**, *1862* (2), 324−334.
(5) Shi, Y. A Glimpse of Structural Biology through X-Ray Crystallography. *Cell* **2014**, *159* (5), 995−1014.
(6) Zheng, H.; Handing, K. B.; Zimmerman, M. D.; Shabalin, I. G.; Almo, S. C.; Minor, W. X-ray crystallography over the past decade for novel drug discovery - where are we heading next? *Expert Opin. Drug Discovery* **2015**, *10* (9), 975−989.
(7) Markwick, P. R. L.; Malliavin, T.; Nilges, M. Structural biology by NMR: structure, dynamics, and interactions. *PLoS Comput. Biol.* **2008**, *4* (9), No. e1000168.
(8) van der Wel, P. C. A. New applications of solid-state NMR in structural biology. *Emerg. Top. Life Sci.* **2018**, *2* (1), 57−67.
(9) Bolla, J. R.; Agasid, M. T.; Mehmood, S.; Robinson, C. V. Membrane Protein-Lipid Interactions Probed Using Mass Spectrometry. *Annu. Rev. Biochem.* **2019**, *88*, 85−111.
(10) Lyu, J.; Liu, Y.; McCabe, J. W.; Schrecke, S.; Fang, L.; Russell, D. H.; Laganowsky, A. Discovery of Potent Charge-Reducing Molecules for Native Ion Mobility Mass Spectrometry Studies. *Anal. Chem.* **2020**, *92* (16), 11242−11249.
(11) McCabe, J. W.; Mallis, C. S.; Kocurek, K. I.; Poltash, M. L.; Shirzadeh, M.; Hebert, M. J.; Fan, L.; Walker, T. E.; Zheng, X.; Jiang, T.; Dong, S.; Lin, C.-W.; Laganowsky, A.; Russell, D. H. First-Principles Collision Cross Section Measurements of Large Proteins and Protein Complexes. *Anal. Chem.* **2020**, *92* (16), 11155−11163.
(12) Poltash, M. L.; McCabe, J. W.; Shirzadeh, M.; Laganowsky, A.; Clowers, B. H.; Russell, D. H. Fourier Transform-Ion Mobility-Orbitrap Mass Spectrometer: A Next-Generation Instrument for Native Mass Spectrometry. *Anal. Chem.* **2018**, *90* (17), 10472−10478.
(13) Poltash, M. L.; McCabe, J. W.; Shirzadeh, M.; Laganowsky, A.; Russell, D. H. Native IM-Orbitrap MS: Resolving what was hidden. *TrAC, Trends Anal. Chem.* **2020**, *124*, 115533.
(14) Poltash, M. L.; Shirzadeh, M.; McCabe, J. W.; Moghadamchargari, Z.; Laganowsky, A.; Russell, D. H. New insights into the metal-induced oxidative degradation pathways of transthyretin. *Chem. Commun.* **2019**, *55* (28), 4091−4094.
(15) Lin, C.-W.; McCabe, J. W.; Russell, D. H.; Barondeau, D. P. Molecular Mechanism of ISC Iron-Sulfur Cluster Biogenesis Revealed by High-Resolution Native Mass Spectrometry. *J. Am. Chem. Soc.* **2020**, *142* (13), 6018−6029.
(16) Silveira, J. A.; Jeon, J.; Gamage, C. M.; Pai, P.-J.; Fort, K. L.; Russell, D. H. Damping Factor Links Periodic Focusing and Uniform Field Ion Mobility for Accurate Determination of Collision Cross Sections. *Anal. Chem.* **2012**, *84* (6), 2818−2824.
(17) McCabe, J. W.; Shirzadeh, M.; Walker, T. E.; Lin, C.-W.; Jones, B. J.; Wysocki, V. H.; Barondeau, D. P.; Clemmer, D. E.; Laganowsky, A.; Russell, D. H. Variable-Temperature Electrospray Ionization for Temperature-Dependent Folding/Refolding Reactions of Proteins and Ligand Binding. *Anal. Chem.* **2021**, *93* (18), 6924−6931.
(18) Brabeck, G. F.; Chen, H.; Hoffman, N. M.; Wang, L.; Reilly, P. T. A. Development of MSn in Digitally Operated Linear Ion Guides. *Anal. Chem.* **2014**, *86* (15), 7757−7763.
(19) Brabeck, G. F.; Koizumi, H.; Koizumi, E.; Reilly, P. T. A. Characterization of quadrupole mass filters operated with frequency-asymmetric and amplitude-asymmetric waveforms. *Int. J. Mass Spectrom.* **2016**, *404*, 8−13.
(20) Brabeck, G. F.; Reilly, P. T. A. Mapping ion stability in digitally driven ion traps and guides. *Int. J. Mass Spectrom.* **2014**, *364*, 1−8.
(21) Brabeck, G. F.; Reilly, P. T. A. Computational Analysis of Quadrupole Mass Filters Employing Nontraditional Waveforms. *J. Am. Soc. Mass Spectrom.* **2016**, *27* (6), 1122−1127.
(22) Hoffman, N. M.; Gotlib, Z. P.; Opačić, B.; Huntley, A. P.; Moon, A. M.; Donahoe, K. E. G.; Brabeck, G. F.; Reilly, P. T. A. Digital Waveform Technology and the Next Generation of Mass Spectrometers. *J. Am. Soc. Mass Spectrom.* **2018**, *29* (2), 331−341.
(23) Hoffman, N. M.; Opačić, B.; Reilly, P. T. A. Note: An inexpensive square waveform ion funnel driver. *Rev. Sci. Instrum.* **2017**, *88* (1), 016104.
(24) Huntley, A. P.; Brabeck, G. F.; Reilly, P. T. A. Tutorial and comprehensive computational study of acceptance and transmission of sinusoidal and digital ion guides. *J. Mass Spectrom.* **2019**, *54* (11), 857−868.
(25) Huntley, A. P.; Brabeck, G. F.; Reilly, P. T. A. Influence of the RF drive potential on the acceptance behavior of pure quadrupole mass filters operated in stability zones A and B. *Int. J. Mass Spectrom.* **2020**, *450*, 116303.
(26) Huntley, A. P.; Opačić, B.; Brabeck, G. F.; Reilly, P. T. A. Simulation of instantaneous changes in ion motion with waveform duty cycle. *Int. J. Mass Spectrom.* **2019**, *441*, 8−13.
(27) Lee, J.; Marino, M. A.; Koizumi, H.; Reilly, P. T. A. Simulation of duty cycle-based trapping and ejection of massive ions using linear digital quadrupoles: The enabling technology for high resolution time-of-flight mass spectrometry in the ultra high mass range. *Int. J. Mass Spectrom.* **2011**, *304* (1), 36−40.

(28) Opačić, B.; Hoffman, N. M.; Gotlib, Z. P.; Clowers, B. H.; Reilly, P. T. A. Using Digital Waveforms to Mitigate Solvent Clustering During Mass Filter Analysis of Proteins. *J. Am. Soc. Mass Spectrom.* **2018**, *29* (10), 2081−2085.
(29) Opačić, B.; Huntley, A. P.; Clowers, B. H.; Reilly, P. T. A. Digital mass filter analysis in stability zones A and B. *J. Mass Spectrom.* **2018**, *53* (12), 1155−1168.
(30) Reece, M. E.; Huntley, A. P.; Moon, A. M.; Reilly, P. T. A. Digital Mass Analysis in a Linear Ion Trap without Auxiliary Waveforms. *J. Am. Soc. Mass Spectrom.* **2020**, *31* (1), 103−108.
(31) Reilly, P. T. A.; Brabeck, G. F. Mapping the pseudopotential well for all values of the Mathieu parameter q in digital and sinusoidal ion traps. *Int. J. Mass Spectrom.* **2015**, *392*, 86−90.
(32) Singh, R.; Jayaram, V.; Reilly, P. T. A. Duty cycle-based isolation in linear quadrupole ion traps. *Int. J. Mass Spectrom.* **2013**, *343*−*344*, 45−49.
(33) Shirzadeh, M.; Boone, C. D.; Laganowsky, A.; Russell, D. H. Topological Analysis of Transthyretin Disassembly Mechanism: Surface-Induced Dissociation Reveals Hidden Reaction Pathways. *Anal. Chem.* **2019**, *91* (3), 2345−2351.
(34) Snyder, D. T.; Panczyk, E.; Stiving, A. Q.; Gilbert, J. D.; Somogyi, A.; Kaplan, D.; Wysocki, V. Design and Performance of a Second-Generation Surface-Induced Dissociation Cell for Fourier Transform Ion Cyclotron Resonance Mass Spectrometry of Native Protein Complexes. *Anal. Chem.* **2019**, *91* (21), 14049−14057.
(35) Stiving, A. Q.; VanAernum, Z. L.; Busch, F.; Harvey, S. R.; Sarni, S. H.; Wysocki, V. H. Surface-Induced Dissociation: An Effective Method for Characterization of Protein Quaternary Structure. *Anal. Chem.* **2019**, *91* (1), 190−209.
(36) VanAernum, Z. L.; Gilbert, J. D.; Belov, M. E.; Makarov, A. A.; Horning, S. R.; Wysocki, V. H. Surface-Induced Dissociation of Noncovalent Protein Complexes in an Extended Mass Range Orbitrap Mass Spectrometer. *Anal. Chem.* **2019**, *91* (5), 3611−3618.
(37) Zhou, M.; Wysocki, V. H. Surface Induced Dissociation: Dissecting Noncovalent Protein Complexes in the Gas phase. *Acc. Chem. Res.* **2014**, *47* (4), 1010−1018.
(38) Zhurov, K. O.; Fornelli, L.; Wodrich, M. D.; Laskay, Ü. A.; Tsybin, Y. O. Principles of electron capture and transfer dissociation mass spectrometry applied to peptide and protein structure analysis. *Chem. Soc. Rev.* **2013**, *42* (12), 5014−5030.
(39) Fornelli, L.; Srzentić, K.; Toby, T. K.; Doubleday, P. F.; Huguet, R.; Mullen, C.; Melani, R. D.; dos Santos Seckler, H.; DeHart, C. J.; Weisbrod, C. R.; Durbin, K. R.; Greer, J. B.; Early, B. P.; Fellers, R. T.; Zabrouskov, V.; Thomas, P.; Compton, P. D.; Kelleher, N. L. Thorough performance evaluation of 213 nm ultraviolet photodissociation for top-down proteomics. *Mol. Cell. Proteomics* **2020**, *19*, 405.
(40) Brodbelt, J. S. Photodissociation mass spectrometry: new tools for characterization of biological molecules. *Chem. Soc. Rev.* **2014**, *43* (8), 2757−2783.
(41) Weaver, J.; Jiang, M.; Roth, A.; Puchalla, J.; Zhang, J.; Rye, H. S. GroEL actively stimulates folding of the endogenous substrate protein PepQ. *Nat. Commun.* **2017**, *8* (1), 15934.
(42) Cong, X.; Liu, Y.; Liu, W.; Liang, X.; Russell, D. H.; Laganowsky, A. Determining Membrane Protein-Lipid Binding Thermodynamics Using Native Mass Spectrometry. *J. Am. Chem. Soc.* **2016**, *138* (13), 4346−9.
(43) Laganowsky, A.; Reading, E.; Hopper, J. T. S.; Robinson, C. V. Mass spectrometry of intact membrane protein complexes. *Nat. Protoc.* **2013**, *8* (4), 639−651.
(44) Patrick, J. W.; Boone, C. D.; Liu, W.; Conover, G. M.; Liu, Y.; Cong, X.; Laganowsky, A. *Proc. Natl. Acad. Sci. U. S. A.* **2018**, *115* (12), 2976−2981.
(45) Poltash, M. L.; McCabe, J. W.; Patrick, J. W.; Laganowsky, A.; Russell, D. H. Development and Evaluation of a Reverse-Entry Ion Source Orbitrap Mass Spectrometer. *J. Am. Soc. Mass Spectrom.* **2019**, *30* (1), 192−198.
(46) Knorr, F. J.; Eatherton, R. L.; Siems, W. F.; Hill, H. H. Fourier Transform Ion Mobility Spectrometry. *Anal. Chem.* **1985**, *57* (2), 402−406.
(47) Kwantwi-Barima, P.; Reinecke, T.; Clowers, B. H. Increased ion throughput using tristate ion-gate multiplexing. *Analyst* **2019**, *144* (22), 6660−6670.
(48) Morrison, K. A.; Siems, W. F.; Clowers, B. H. Augmenting Ion Trap Mass Spectrometers Using a Frequency Modulated Drift Tube Ion Mobility Spectrometer. *Anal. Chem.* **2016**, *88* (6), 3121−3129.
(49) Reinecke, T.; Davis, A. L.; Clowers, B. H. Determination of Gas-Phase Ion Mobility Coefficients Using Voltage Sweep Multiplexing. *J. Am. Soc. Mass Spectrom.* **2019**, *30* (6), 977−986.
(50) Reinecke, T.; Naylor, C. N.; Clowers, B. H. Ion multiplexing: Maximizing throughput and signal to noise ratio for ion mobility spectrometry. *TrAC, Trends Anal. Chem.* **2019**, *116*, 340−345.
(51) Sanders, J. D.; Butalewicz, J. P.; Clowers, B. H.; Brodbelt, J. S. Absorption Mode Fourier Transform Ion Mobility Mass Spectrometry Multiplexing Combined with Half-Window Apodization Windows Improves Resolution and Shortens Acquisition Times. *Anal. Chem.* **2021**, *93* (27), 9513−9520.
(52) Schoen, A. E.; Amy, J. W.; Ciupek, J. D.; Cooks, R. G.; Dobberstein, P.; Jung, G. A hybrid BEQQ mass spectrometer. *Int. J. Mass Spectrom. Ion Processes* **1985**, *65* (1), 125−140.
(53) Alexander, W. M.; Ficarro, S. B.; Adelmant, G.; Marto, J. A. multiplierz v2.0: A Python-based ecosystem for shared access and analysis of native mass spectrometry data. *Proteomics* **2017**, *17* (15−16), 1700091.
(54) Virtanen, P.; Gommers, R.; Oliphant, T. E.; Haberland, M.; Reddy, T.; Cournapeau, D.; Burovski, E.; Peterson, P.; Weckesser, W.; Bright, J.; van der Walt, S. J.; Brett, M.; Wilson, J.; Millman, K. J.; Mayorov, N.; Nelson, A. R. J.; Jones, E.; Kern, R.; Larson, E.; Carey, C J; Polat, I.; Feng, Y.; Moore, E. W.; VanderPlas, J.; Laxalde, D.; Perktold, J.; Cimrman, R.; Henriksen, I.; Quintero, E. A.; Harris, C. R.; Archibald, A. M.; Ribeiro, A. H.; Pedregosa, F.; van Mulbregt, P.; Vijaykumar, A.; Bardelli, A. P.; Rothberg, A.; Hilboll, A.; Kloeckner, A.; Scopatz, A.; Lee, A.; Rokem, A.; Woods, C. N.; Fulton, C.; Masson, C.; Haggstrom, C.; Fitzgerald, C.; Nicholson, D. A.; Hagen, D. R.; Pasechnik, D. V.; Olivetti, E.; Martin, E.; Wieser, E.; Silva, F.; Lenders, F.; Wilhelm, F.; Young, G.; Price, G. A.; Ingold, G.-L.; Allen, G. E.; Lee, G. R.; Audren, H.; Probst, I.; Dietrich, J. P.; Silterra, J.; Webber, J. T; Slavic, J.; Nothman, J.; Buchner, J.; Kulick, J.; Schonberger, J. L.; de Miranda Cardoso, J. V.; Reimer, J.; Harrington, J.; Rodriguez, J. L. C.; Nunez-Iglesias, J.; Kuczynski, J.; Tritz, K.; Thoma, M.; Newville, M.; Kummerer, M.; Bolingbroke, M.; Tartre, M.; Pak, M.; Smith, N. J.; Nowaczyk, N.; Shebanov, N.; Pavlyk, O.; Brodtkorb, P. A.; Lee, P.; McGibbon, R. T.; Feldbauer, R.; Lewis, S.; Tygier, S.; Sievert, S.; Vigna, S.; Peterson, S.; More, S.; Pudlik, T.; Oshima, T.; Pingel, T. J.; Robitaille, T. P.; Spura, T.; Jones, T. R.; Cera, T.; Leslie, T.; Zito, T.; Krauss, T.; Upadhyay, U.; Halchenko, Y. O.; Vazquez-Baeza, Y. SciPy 1.0: fundamental algorithms for scientific computing in Python. *Nat. Methods* **2020**, *17* (3), 261−272.
(55) van der Walt, S.; Colbert, S. C.; Varoquaux, G. The NumPy Array: A Structure for Efficient Numerical Computation. *Comput. Sci. Eng.* **2011**, *13* (2), 22−30.
(56) Marty, M. T.; Baldwin, A. J.; Marklund, E. G.; Hochberg, G. K. A.; Benesch, J. L. P.; Robinson, C. V. Bayesian Deconvolution of Mass and Ion Mobility Spectra: From Binary Interactions to Polydisperse Ensembles. *Anal. Chem.* **2015**, *87* (8), 4370−4376.
(57) Bern, M.; Caval, T.; Kil, Y. J.; Tang, W.; Becker, C.; Carlson, E.; Kletter, D.; Sen, K. I.; Galy, N.; Hagemans, D.; Franc, V.; Heck, A. J. R. Parsimonious Charge Deconvolution for Native Mass Spectrometry. *J. Proteome Res.* **2018**, *17* (3), 1216−1226.
(58) Reilly, P. T. A.; Chakravorty, S.; Bailey, C. F.; Obe, F. O.; Huntley, A. P. Will the Digital Mass Filter Be the Next High-Resolution High-Mass Analyzer? *J. Am. Soc. Mass Spectrom.* **2021**, *32* (10), 2615−2620.
(59) Mallis, C. S.; Zheng, X.; Qiu, X.; McCabe, J. W.; Shirzadeh, M.; Lyu, J.; Laganowsky, A.; Russell, D. H. Development of native MS

capabilities on an extended mass range Q-TOF MS. *Int. J. Mass Spectrom.* **2020**, *458*, 116451.
(60) Campuzano, I. D. G.; Li, H.; Bagal, D.; Lippens, J. L.; Svitel, J.; Kurzeja, R. J. M.; Xu, H.; Schnier, P. D.; Loo, J. A. Native MS Analysis of Bacteriorhodopsin and an Empty Nanodisc by Orthogonal Acceleration Time-of-Flight, Orbitrap and Ion Cyclotron Resonance. *Anal. Chem.* **2016**, *88* (24), 12427−12436.
(61) Allison, T. M.; Reading, E.; Liko, I.; Baldwin, A. J.; Laganowsky, A.; Robinson, C. V. Quantifying the stabilizing effects of protein-ligand interactions in the gas phase. *Nat. Commun.* **2015**, *6* (1), 8551.
(62) Laganowsky, A.; Reading, E.; Allison, T. M.; Ulmschneider, M. B.; Degiacomi, M. T.; Baldwin, A. J.; Robinson, C. V. Membrane proteins bind lipids selectively to modulate their structure and function. *Nature* **2014**, *510* (7503), 172−175.
(63) Liu, Y.; Cong, X.; Liu, W.; Laganowsky, A. Characterization of Membrane Protein-Lipid Interactions by Mass Spectrometry Ion Mobility Mass Spectrometry. *J. Am. Soc. Mass Spectrom.* **2017**, *28* (4), 579−586.
(64) Patrick, J. W.; Laganowsky, A. Generation of Charge-Reduced Ions of Membrane Protein Complexes for Native Ion Mobility Mass Spectrometry Studies. *J. Am. Soc. Mass Spectrom.* **2019**, *30*, 886.
(65) Patrick, J. W.; Laganowsky, A. Probing Heterogeneous Lipid Interactions with Membrane Proteins Using Mass Spectrometry. *Methods Mol. Biol.* **2019**, *2003*, 175−190.
(66) Schrecke, S.; Zhu, Y.; McCabe, J. W.; Bartz, M.; Packianathan, C.; Zhao, M.; Zhou, M.; Russell, D.; Laganowsky, A. Selective regulation of human TRAAK channels by biologically active phospholipids. *Nat. Chem. Biol.* **2021**, *17* (1), 89−95.
(67) Keener, J. E.; Zhang, G.; Marty, M. T. Native Mass Spectrometry of Membrane Proteins. *Anal. Chem.* **2021**, *93* (1), 583−597.
(68) van Duijn, E.; Simmons, D. A.; van den Heuvel, R. H. H.; Bakkes, P. J.; van Heerikhuizen, H.; Heeren, R. M. A.; Robinson, C. V.; van der Vies, S. M.; Heck, A. J. R. Tandem Mass Spectrometry of Intact GroEL-Substrate Complexes Reveals Substrate-Specific Conformational Changes in the trans Ring. *J. Am. Chem. Soc.* **2006**, *128* (14), 4694−4702.
(69) Stiving, A. Q.; Jones, B. J.; Ujma, J.; Giles, K.; Wysocki, V. H. Collision Cross Sections of Charge-Reduced Proteins and Protein Complexes: A Database for Collision Cross Section Calibration. *Anal. Chem.* **2020**, *92* (6), 4475−4483.
(70) Aquilina, J. A.; Benesch, J. L. P.; Bateman, O. A.; Slingsby, C.; Robinson, C. V. Polydispersity of a mammalian chaperone: Mass spectrometry reveals the population of oligomers in αB-Crystallin. *Proc. Natl. Acad. Sci. U. S. A.* **2003**, *100* (19), 10611−10616.
(71) Hunt, D. F.; Yates, J. R.; Shabanowitz, J.; Winston, S.; Hauer, C. R. Protein sequencing by tandem mass spectrometry. *Proc. Natl. Acad. Sci. U. S. A.* **1986**, *83* (17), 6233−6237.
(72) Fellers, R. T.; Greer, J. B.; Early, B. P.; Yu, X.; LeDuc, R. D.; Kelleher, N. L.; Thomas, P. M. ProSight Lite: Graphical software to analyze top-down mass spectrometry data. *Proteomics* **2015**, *15* (7), 1235−1238.
(73) Michalski, A.; Damoc, E.; Hauschild, J.-P.; Lange, O.; Wieghaus, A.; Makarov, A.; Nagaraj, N.; Cox, J.; Mann, M.; Horning, S. Mass Spectrometry-based Proteomics Using Q Exactive, a High-performance Benchtop Quadrupole Orbitrap Mass Spectrometer. *Mol. Cell. Proteomics* **2011**, *10* (9), M111.011015.

https://doi.org/10.1021/jasms.1c00245
J. Am. Soc. Mass Spectrom. 2021, 32, 2812−2820